Food Processing Operations Modeling
Design and Analysis

edited by
Joseph Irudayaraj
The Pennsylvania State University
University Park, Pennsylvania

MARCEL DEKKER, INC. NEW YORK • BASEL

7 Infrared Heating of Biological Materials

Oladiran O. Fasina
U.S. Department of Agriculture–Agricultural Research Service and North Carolina State University, Raleigh, North Carolina

Robert Thomas Tyler
University of Saskatchewan, Saskatoon, Canada

1 INTRODUCTION

Infrared refers broadly to that portion of the electromagnetic spectrum starting at the deep red (the point at which light just begins to become visible, hence the name infrared) and extending to the microwave radar region. As shown in Figure 1, the relative position of infrared region of the electromagnetic spectrum is in the wavelength range of 0.75 to 1000 μm. Infrared waves are described as short, medium, or long wave. Short infrared waves (or near infrared) are closest to visible light. Because much of this energy is light, it is easily reflected. Short infrared waves occupy the region of the electromagnetic spectrum in the wavelength between 0.75 and 3.0 μm. The long infrared (or far infrared) waves, spanning the wavelength region of 25–1000 μm, are readily absorbed by most materials as heat. The medium waves (or middle infrared) occupy the region between the short infrared and long infrared regions [1].

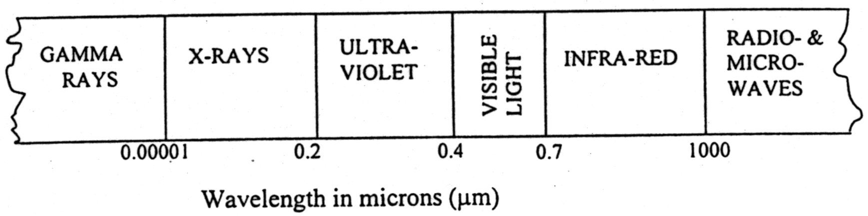

FIGURE 1 The electromagnetic spectrum.

When radiant electromagnetic energy impinges upon a food surface, it may induce changes in the electronic, vibrational, or rotational states of atoms and molecules [2]. The types of mechanisms for energy absorption are determined by the wavelength range of the incident energy. Changes in the electronic state correspond to wavelengths in the range between 0.2 and 0.7 μm (ultraviolet and visible rays); changes in the vibrational state correspond to wavelengths in the range 2.5–100 μm (part of infrared region); and changes in the rotational state correspond to wavelengths above 100 μm (microwaves). Infrared radiation causes molecular vibration changes; hence, heating occurs when biological materials are exposed to infrared radiation.

The fundamental relationships of infrared energy are established by three basic laws [Eqs. (1)–(3)] that determine the distribution and quantity of infrared energy. The laws are written for a blackbody, which assumes that a surface will absorb all and reflect none of the radiation falling on it. An ideal "blackbody" is a surface that absorbs and in turn radiates all the energy incident upon it.

Stefan–Boltzmann Law

$$W = \sigma T_{ab}^4 \tag{1}$$

Wien's Displacement Law

$$\lambda_{max} = \frac{2897.6}{T_{ab}} \tag{2}$$

Planck's Equation

$$E = \frac{C_1 \lambda^{-5}}{\exp(C_2/\lambda T) - 1} \tag{3}$$

where the first (C_1) and second (C_2) radiation constants have values of 3.742×10^8 W μm^4/m^2 and 1.469 μm K, respectively. The symbols are defined in Section 6 nomenclature.

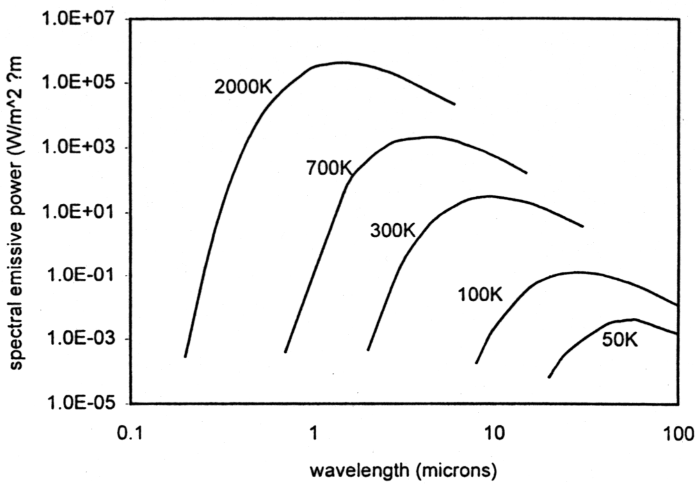

FIGURE 2 Spectral blackbody emissive power.

The Stefan–Boltzmann law and Planck's equation provide the means for determining the intensity and spectral distribution of the emission from a radiator. The Stefan–Boltzmann law shows that the intensity of heat at the surface of a body exposed to infrared radiation is proportional to the fourth power of temperature. The Wein's displacement law states that the peak wavelength (λ_{max}) varies inversely with the absolute temperature of the radiating object. Figure 2 shows the emissive power curves of blackbody radiation versus wavelengths at different temperatures. The hotter the object, the shorter the wavelength of infrared radiation. The total emitted energy is the integral or the area under the curve shown in Figure 2 and can be calculated using the Stefan–Boltzmann relationship.

Because no object is a perfect emitter (i.e., a blackbody), real substances are characterized by an efficacy of radiant emission called emittance or emissivity (ε). The radiant energy flux for real objects is then calculated from

$$W = \varepsilon \sigma T_{ab}^4 \tag{4}$$

Emissivity varies with wavelength and temperature. The common practice in engineering, however, is to represent the emissivity for the entire band of the electromagnetic spectrum involved rather than for a particular wavelength. Emissivity data for biological materials is scarce. Typical values of emissivity for agricultural crops vary from 0.7 to 0.9 [3,4]. Where there are no data for a particular application, an emissivity value of 0.9 is often used.

2 INFRARED HEAT GENERATION

Most generators of infrared energy are either electrically heated or gas fired. The electrical generators of infrared radiation include quartz lamp, tungsten arc lamp, xenon arc lamp, nonsheathed radiator, and resistance element (Table 1). For electrically heated radiators, infrared radiation is obtained by passing an electric current through an element [6]. Quartz, tungsten, and xenon lamps generally have maximum radiation at wavelength less than 1.3 μm. They are therefore referred to as light (short-wave) radiators. These lamps emit at temperatures of 1773–2073 K [7]. Resistance elements and gas-type generators are generally dark (long-wave) radiators because they have maximum radiation in the invisible infrared rays (> 1.3 μm). Gas-fired generators are made of perforated plate (metal or refractory) that is heated by gas flames in one of the surfaces, thereby causing the plate to rise in temperature and emits radiant energy [8]. The characteristics of commercially used infrared heat sources are compared in Table 1 [5].

3 APPLICATIONS TO BIOLOGICAL MATERIALS

Sun drying is the oldest method that has been used to dry agricultural products. Because most of the radiant energy of the sun is in the infrared region, infrared energy is indirectly the oldest and most traditional energy source for agricultural applications. Despite the historical nature of infrared energy in food preservation, the use of infrared radiation is mostly at the industrial level, such as in drying of coatings (powders, paints, inks, adhesives, films), in hazardous heating (space heating for oil and gas and petrochemical industries) and in electronics and metal processing applications.

Interest in the use of infrared heating in food processing has increased in the past few years due to recent developments in the design of infrared heaters that offer rapid and economical methods for production of food products with high organoleptic and nutritional value. The most significant advantage of infrared drying when used for drying is the reduction in drying time. Other advantages of infrared heating include the following [2,8]:

(a) High efficiency to convert electrical energy into heat when electric heaters are used.
(b) Efficient heat transfer to the food reduces processing time and energy costs.

TABLE 1 Characteristics of Commercially Used Infrared Heat Sources

Infrared source		Source temperature: Usual range (K)	Source temperature: Max (K)	Peak wavelength (μm)	Power (kW/m²)
Electrically heated radiators					
Nonsheathed radiators	Sylite	1,750–1,800	2,200	1.65	Up to 80
	Graphite	2,300–2,800	3,500	1.2	Up to 1200
	Metallic–filament tungsten	1,900–2,200	2,700	1.2	$(1–1.4) \times 10^5$
	Metallic–molybednum	1,600–2,000	2,000	0.9	$(1–2) \times 10^5$
Sheathed radiators	Light bulbs	1,900–2,500	2,500	1.3	Up to 20
	Quarta lamp	1,900–2,500	2,800	1.0	30–400
	Plate radiators	700–1,200	1,200	4.0–9.0	4–14
	Xenon arc lamp	5,000–10,000	10,000	0.8–1.1	Up to 50
	Tungsten arc lamp	3,200–4,000	7,000	0.72	Up to 1400
Gas-heated					
Flame	Direct flame (Bunsen, Teclu, or Mecker burner)	500–1,600	1,800	2.8–4.3	20–30
	Indirect flame—ceramic element	600–800	1,500	4.0	50–60
	Indirect flame—metallic element	300–900	1,000	3.6	20–30
Flameless	Heated porous plate with internal burning	350–850	1,200	4.0	40–90
	Heated porous plate with external burning	1,000–1,700	2,000	1.5–2.0	160–2400

Source: Ref. 5.

(c) The air surrounding the equipment is maintained at ambient level.
(d) Infrared heaters are less expensive when compared to dielectric and microwave sources and they have longer service life and low maintenance.
(e) Surface irregularities on foods have insignificant effect on infrared heating—uniform heating of product is easily achieved.

Some of the disadvantages of infrared heating are (a) proper scaling up of heaters from laboratory model to full-plant model, and (b) infrared heating is essentially a surface heating method and is therefore best for thin materials.

Infrared heat is generally applied to biological materials in order to achieve thermal effects such as controlling insect infestation in stored product, inactivation of toxic and antimicrobial factors and degradative enzymes, reduction of microbial counts, enhancement of the dehulling of legume grains, and starch gelatinization in starch bearing materials [7,9–10]. The determination of appropriate equations to describe a process requires an understanding of the physical, chemical, and microbiological changes that occur when the process is applied to biological materials. In this section, some of the applications of infrared heating in food and agricultural industries are discussed. Examples of the various changes that occur in infrared heated foods are also presented.

3.1 Applications Involving Insect Disinfestation

Kirkpatrick [11] showed a 99% death rate of *Sitophilus oryzae* and a 93% death rate of *Rhyzopertha dominica* when insect-infested wheat samples were exposed to infrared radiation. The temperature of the wheat samples increased to 48.6°C. In another study, Kirkpatrick et al. [12] found that the natural infestations of stored wheat by the weevil *S. oryzae*, the grain borer *R. dominica*, *Crypolestes pusillus Schonh*, and *Tribolinum castaneum* were controlled by raising sample temperature to 55°C. Despite these encouraging results, there is no evidence that infrared heating is used commercially to disinfect food and agricultural materials. This is probably due to the limited use of infrared heating in the food industry at the time these studies were conducted. Due to the energy crisis of the 1970s, it was less expensive for food manufacturers then to use chemicals for food preservation.

3.2 Applications Involving Legume and Oil-Bearing Materials

Most of the commercial use of infrared heat processing in the food industry involves the inactivation of antinutritional factors in legume seeds (mostly

soybeans) and enzymes that cause product degradation and development of rancidity. Several studies carried out by researchers at the Agricultural University in Wageningen, the Netherlands [13–16], showed that infrared heating can be used to improve the nutritive value of soybeans. The researchers, in addition to results from other published studies [17–19], found that infrared radiation can be used to inactivate lipoxygenase enzyme (that causes oxidative rancidity), reduce the trypsin inhibitor and other antinutritional factor levels, and increase the binding, emulsion power, water holding capacity, and shelf life of full-fat soybean flour. This has generally led to a longer shelf life of the product. Perhaps the most important conclusion made by the Wageningen researchers is that infrared treatment of soybeans offers the possibility for reducing energy requirements and production costs in comparison to the conventional steam-heating method used for soybean processing. The researchers showed that soybeans can be infrared heated to surface temperatures of 125–133°C for 60 sec. Steam heating is usually carried out at temperatures of 110–125°C for 20–30 min [20–22]. In addition, steam-heated samples have to be dried after treatment thus increasing processing cost.

When cocoa beans were infrared heated prior to dehulling, there was a significant improvement in winnowing performance during the separation of nib or beans from the shell. The shells became lighter due to expansion and are thus more effectively removed during air separation [20–22]. In addition, bacteria and contamination levels were reduced by 95%. The effect of infrared heating on the microbial counts of cocoa nibs is shown in Table 2 [9]. Infrared heating of the nibs was carried out for 10 sec under a ceramic plate heated to 970°C.

Cenkowski and Sosulski [23] investigated the effect of infrared heating on the physical and cooking properties of lentils. They found that cooking time was shortened from 30 mm for the controlled seeds to 15 mm for lentils adjusted to 25.8% moisture content and infrared heated to 55°C. Infrared

Table 2 Effect of Infrared Treatment of Cocoa Nibs on Microbial Counts

	Before infrared treatment (counts/g)	After infrared treatment (counts/g)
Total count	5×10^6	2×10^5
Enterobacteria	10^4	10
Yeasts	8×10^4	$<10^2$
Molds	6×10^4	$<10^2$

Source: Ref. 9.

heating was effective in the gelatinization and solubilization of the starch. When maize germ was infrared heated at different temperatures (98–118°C), the degree of starch gelatinization and water absorption increased and the protein dispersibility and enzyme activity decreased with higher infrared temperatures [24]. The processed wheat germ samples were able to keep for 12 months before any appreciable change in rancidity (free fatty acid [FFA] and peroxide value) occurred.

Fasina et al. [25] investigated the effect of infrared heat treatment on the physical, chemical, mechanical, and functional characteristics of five legume seeds (kidney beans, green peas, black beans, lentil, and pinto beans). Within a duration of 15 sec or less, the seeds were heated to a surface temperature of 140°C. Significant changes (Table 3) in the properties of the seeds in terms of increased volume, lower rupture point and toughness, higher water uptake, and higher leaching losses (when seeds were soaked in water) were obtained in comparison to unprocessed seeds. The changes in the physical and mechanical properties of the seeds were attributed to seed cracking during infrared heating. The authors also found the functionality of the flour (pasting characteristics and protein solubility)

TABLE 3 Water Uptake and Loss of Solubles When Raw and Heated Legume Seeds Were Soaked in Water

Legume sample	Absorbed moisture (g/100 g seed)	LL[a] (g/100 g seed)
Kidney beans		
Raw	133.6	1.1
Processed	137.5	10.3
Green peas		
Raw	119.8	5.5
Processed	118.2	11.0
Black beans		
Raw	130.7	1.7
Processed	144.3	11.1
Lentil		
Raw	136.4	2.5
Processed	140.3	11.5
Pinto bean		
Raw	130.8	3.3
Processed	141.7	11.7

[a] Leaching losses
Source: Ref. 25.

TABLE 4 Pasting Characteristics of Flours from Raw and Infrared-Heated Legume Seeds

Legume sample	Peak height (BU[a])	95°C height (BU)	15 min height (BU)	50°C height (BU)
Kidney bean				
Raw	180	10	60	180
Processed	220	20	120	220
Green pea				
Raw	30	10	20	30
Processed	120	10	100	120
Black bean				
Raw	50	10	20	50
Processed	280	40	120	280
Lentil				
Raw	540	200	360	520
Processed	420	300	410	420
Pinto bean				
Raw	100	20	100	80
Processed	460	60	220	400

[a] BU-Brabender unit.
Source: Ref. 25.

from infrared-heated seeds were superior to those of flour from unprocessed seeds. Table 4 shows the improvement in pasting characteristics of flour from infrared-heated legume seeds; Figure 3 shows the change in protein solubility of the legume seeds due to infrared heating.

3.3 Applications Involving Cereal Grains

The most common reason for applying infrared heating to cereal grains is to gelatinize the starch in them [27–32]. The processed grains are often used in the production of ready-to-eat breakfast cereals, as cereal adjunct in the brewing industry, or as livestock feed. However, there is no substantial evidence showing that significant improvement is obtained when infrared heated cereal grains are fed to livestock [33–35]. Other changes that are achieved when cereal grains are infrared heated include reduction in protein solubility [26, 36], inactivation of peroxidase enzyme in oat flakes [37], reduction of microbial counts on edible wheat bran [38], and reduction of tannin content in sorghum [39]. Figures 4–7 and Tables 5–7 show the changes in the physical and functional characteristics of hull-less and pearled barley infrared heated at different temperatures and moisture content [32].

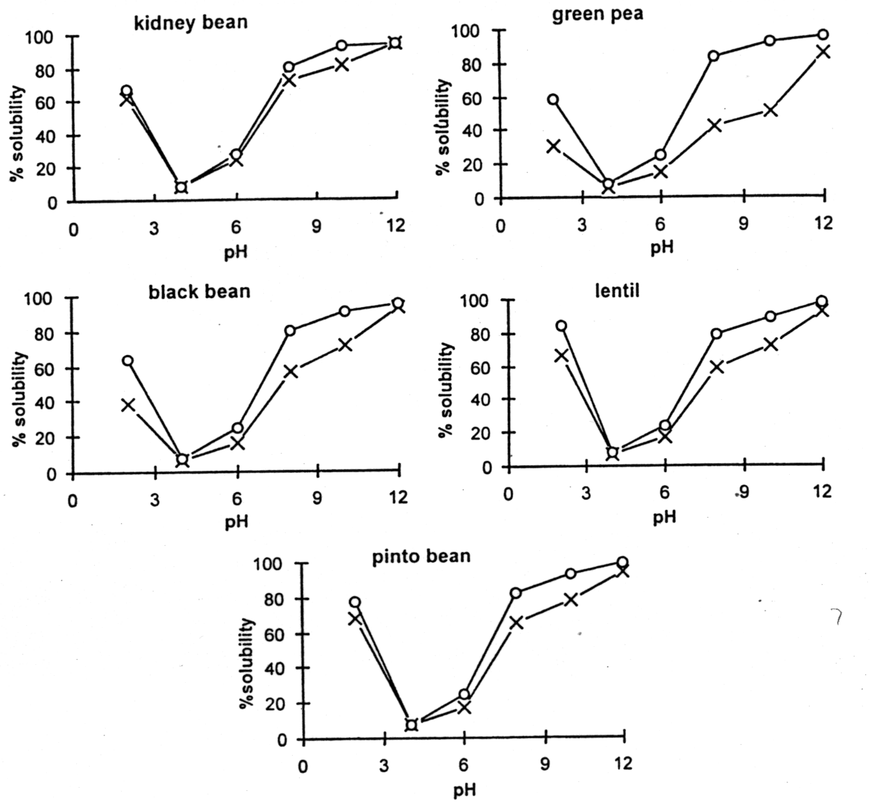

FIGURE 3 Protein insolubility(percent) of legume seeds infrared heated at 140°C ○: unprocessed; ×: processed. (From Ref. 26.)

3.4 Other Applications

In the last decade, there has been increased diversity in the use of infrared radiation in the food industry. Some of the studies that have been reported in the literature include pasteurization of packaged foods [1], heating of oysters and eggs [2], thawing of frozen foods [9], drying of various agricultural materials [40,41], surface sterilization of vegetables [42], enhancement of value of tofu and soy milk [43], and browning of foods [44]. Infrared lamps are now integral parts of buffet tables and cafeteria lines because they are used to keep food hot and to give food a rich red color while under the lamps [28]. Infrared lamps are also used in poultry barns as a heat source for brooding chicks and turkey poults.

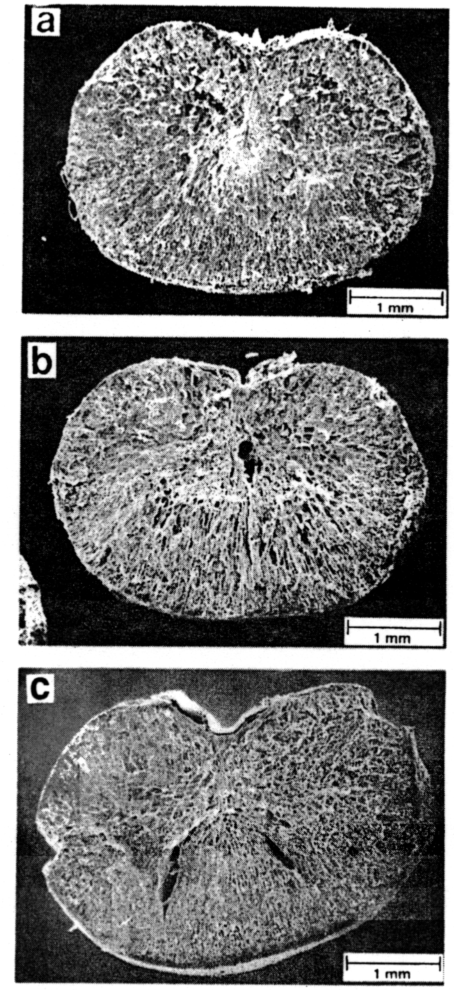

FIGURE 4 Scanning electron micrographs of cross sections of hull-less barley showing kernel expansion due to micronization: (a) unprocessed; (b) initial moisture content of 13.3%, temperature of 150°C; (c) initial moisture content of 26.5%, temperature of 115°C. (From Ref. 32.)

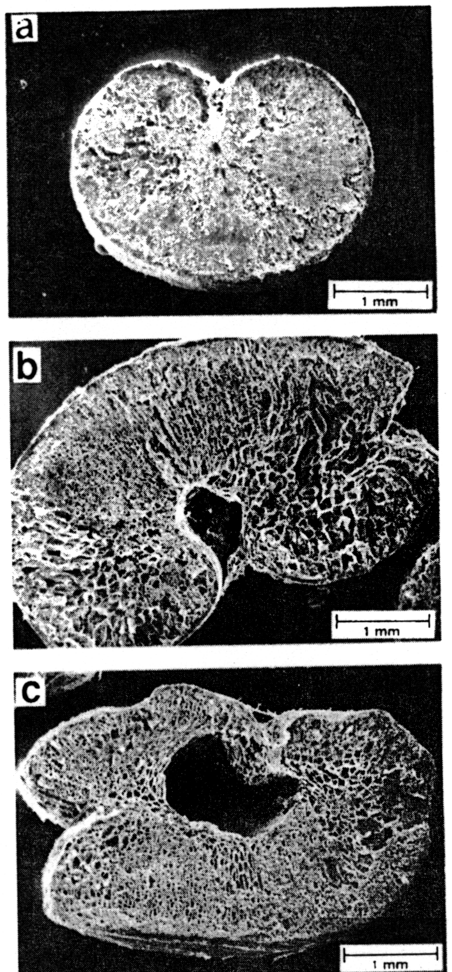

Figure 5 Scanning electron micrographs of cross sections of pearled barley showing kernel expansion due to micronization: (a) unprocessed; (b) initial moisture content of 12.2%, temperature of 150°C; (c) initial moisture content of 25.9%, temperature of 115°C. (From Ref. 32.)

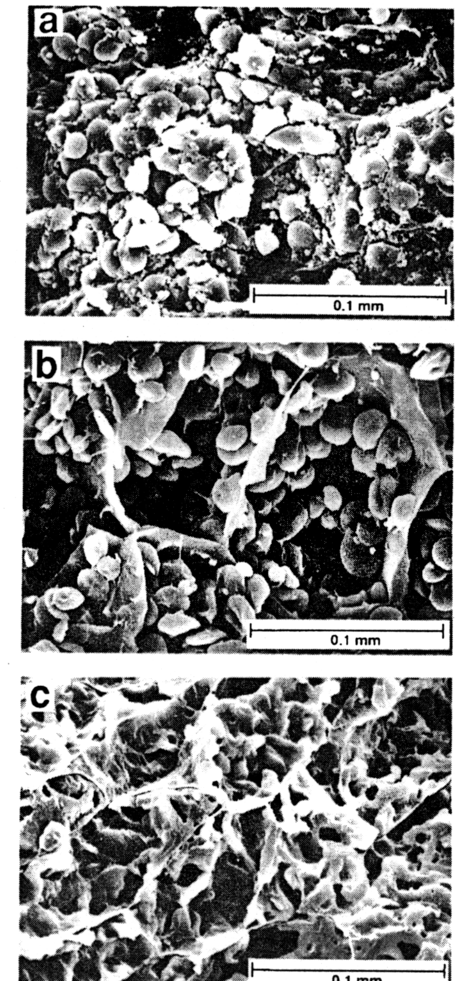

Figure 6 Scanning electron micrographs of cross sections of hull-less barley showing changes in microstructure due to micronization: (a) unprocessed; (b) initial moisture content of 13.3%, temperature of 150°C; (c) initial moisture content of 26.5%, temperature of 115°C. (From Ref. 32.)

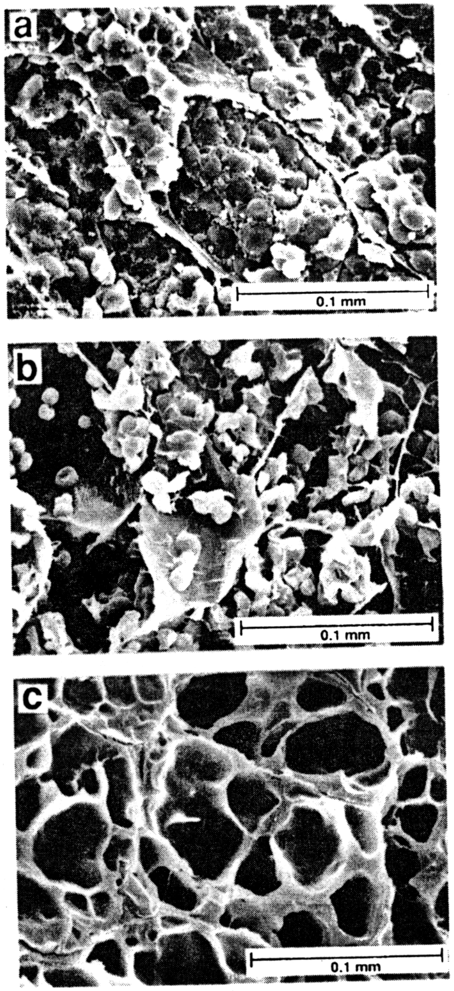

FIGURE 7 Scanning electron micrographs of cross sections of pearled barley showing changes in microstructure due to micronization: (a) unprocessed; (b) initial moisture content of 12.2%, temperature of 150°C; (c) initial moisture content of 25.9%, temperature of 115°C. (From Ref. 32.)

TABLE 5 Percent Amount of Starch Gelatinized[a] in Hull-less and Pearled Barley Samples During Infrared Heating

	Hull-less		Pearled	
Kernel surface temp. (°C)	Initial m.c.[b] (%, w.b.[c])	Gelatinized starch (%)	Initial m.c. (%, w.b.)	Gelatinized starch (%)
115		1.5		0.1
135	13.3[d]	11.2	12.2[d]	2.9
150		47.4		14.0
105		14.3		1.9
115	19.2	34.3	19.3	20.5
135		85.3		44.8
105	26.5	84.1	25.9	26.5
115		93.8		67.3

[a] Maximum deviation of 0.8 from mean values.
[b] m.c. = moisture content.
[c] w.b. = wet
[d] Unconditioned.
Source: Ref. 32.

TABLE 6 Thermal Parameters for Infrared-Heated Hull-less and Pearled Barley Flours Showing the Effect of Kernel Surface Temperature

Temp. (°C)	Hull-less T_p (°C)	ΔH (J/g)	Pearled T_p (°C)	ΔH (J/g)
Raw	67.6	8.02	65.0	7.58
115	67.3	7.80	65.1	7.47
135	67.3	7.30	65.1	7.23
150	67.3	4.85	66.1	6.93

Note: Kernels had initial moisture contents of 12.2%.
Source: Ref. 25.

Even though this is not the focus of this chapter, we should mention that a major use of infrared radiation in the food industry is in the area of analytical measurements. Modern analytical instrumentations that are based on infrared energy measurements are being used for rapid and routine analyses that are needed in the formulation, quality control and development of food products.

TABLE 7 Water Hydration Capacities (WHC)[a] of Flours from Infrared-Heated Hull-less and Pearled Barley

Kernel surface temp. (ωC)	Hull-less		Pearled	
	Initial m.c.[b] (%, w.b)	WHC (%)	Initial m.c. (%, w.b.)	WHC (%)
Unprocessed		272.2		241.8
115		319.7		261.9
135	13.3[d]	326.8	12.2[d]	300.8
150		429.3		288.8
105		330.8		276.4
115	19.2	347.9	19.3	329.4
135		642.4		434.9
105	26.5	760.1	25.9	356.1
115		857.1		497.6

[a] Maximum deviation of 9.3 from mean values.
[b] m.c. = moisture 8 content.
[c] w.b. = wet basis.
[d] unconditioned.
Source: Ref. 32.

4 MODELING THE INFRARED HEATING OF BIOLOGICAL MATERIALS

4.1 Model Development

As mentioned in the previous sections, infrared heating is becoming an important source of heat treatment in the food industry because of advantages such as simplicity of equipment, fast transient response, significant energy savings, and easy accommodation with convective, conductive, and microwave heating [1]. Factors such as type of raw material (e.g., cereal grain, oil seed, legume), infrared burner temperature, height of infrared burner from the grain bed, residency time of grain under infrared heat, and the initial moisture content of the sample will affect final product temperature and moisture content. The optimum combination of these factors can be obtained by complete experimentation or by the use of computer modeling and simulation with subsequent verification of the models by experimental results. The latter is preferable based on cost and time considerations [45].

Despite the wide application of infrared heating in the food and feed industries, few studies have been reported on transfer of heat and mass in

agricultural crops subjected to this heating method. Zuilichem et al. [9] presented the following set of heat transfer equations to describe the infrared heating of agricultural seeds:

$$\rho c_g \frac{\partial T}{\partial t} = k\left(\frac{\partial^2 T}{\partial r^2} + \frac{2}{r}\frac{\partial T}{\partial r}\right). \tag{5}$$

Equation (5) was solved by applying the Fourier integral and Fourier series to obtain

$$T - T_e = \frac{2h(T_0 - T_e)}{T} \sum_{h=1}^{\infty} \exp(-a\alpha_n^2) \times \frac{A^2\alpha_n^2 + (Ah-1)^2}{\alpha_n^2[A^2\alpha_n^2 + Ah(Ah-1)]} \sin A\alpha_n \sin r\alpha_n \tag{6}$$

where $\alpha_n (n = 1, 2, 3, \ldots)$ are the roots of the equation

$$A\alpha_n \operatorname{cotg}(A\alpha_n) + (Ah - 1) = 0 \tag{7}$$

$$h = \frac{\sigma F(T_e^4 - T_{av}^4)}{k(T_e - T_s)} \tag{8}$$

$$T_{av} = T_i + \frac{\sigma T_e^4}{\rho c_g d} t \tag{9}$$

In developing Eqs. (5)–(9), the authors neglected mass transfer and convection of applied heat to the ambient air surroundings. Parameter F in Eq. (8) was defined as the configuration factor. If this is the case, the calculation of the radiation constant h will be in error because the emissivity of the product is not included in the equation. The appropriate equation to use in the calculation of h (the radiative heat transfer coefficient) will be presented later in this section. Unfortunately, the predictions the authors obtained from these Eqs. (5)–(8) were not validated with experimental results.

There is substantial evidence in the literature indicating that agricultural products experience an increase in temperature and lose moisture when exposed to infrared radiation. Zheng et al. [26] showed that unconditioned legume seeds (initial moisture content 9.5–10%) lose about 2 percentage point of moisture when infrared-heated to a surface temperature of 115°C. When lentil seeds with initial moisture contents of 22.5%, 25.8%, and 38.6% were infrared-heated, the measured final seed temperature were inversely related to initial moisture content [23]. After about 60 sec of infrared heating, the moisture contents of the seeds were respectively reduced to 11%, 13%, and 28%. The corresponding final seed temperature were measured to be 110°C, 125°C, and 130°C. Stephenson and McKee [46] investigated the possibility of using infrared heating for the accelerated drying of oats and barley. The moisture content of oats and barley when infrared-heated to surface temperatures of 100°C and 110°C reduced from 20% to 12.1% for oats and from 17.2% to 11.8% for barley.

As mentioned in Section 1, when an infrared wave impinges on a surface, the molecules at the product surface vibrate at a frequency of 8.8×10^7 to 1.7×10^8 MHz (corresponding to wavelength of 1.8–3.4 μm that is typically used in the food industry). The friction of the intermolecular structure of the product will cause a temperature rise, hence the heating and moisture loss at the surface [47]. Heat passes into the food by conduction and moisture migration to the product surface occurs. Kuang et al. [48] studied the transfer of heat and mass during the use of infrared heating to dry paper. The set of equations used for mass transfer were based on capillary moisture movement. Ratti and Mujumdar [7] presented a set of equations to describe the infrared drying of foodstuff. A lumped moisture model (i.e., no resistance to internal moisture movement) was used to describe the mass transfer component. Numerous studies have shown that the transfer of mass in agricultural crops is mainly a diffusion process [49–51]. In diffusion processes, the mass transfer models take into account the internal and external resistances of the single grain particle to moisture movement [52].

Irudayaraj et al. [53] modeled the drying of cereal grains using two models. The first model assumed that diffusion of moisture occur through vapor and liquid phases within the grain kernel. Luikov's coupled system of partial differential equations [54] for heat and mass transfer in porous media was used to describe the diffusion process. The second model used by the authors assumed that moisture diffuses to the outer boundaries of the kernel in liquid form and that evaporation takes place only at the surface of the grain (conduction model). Simulation results showed that temperature predictions by the Luikov's model approached the equilibrium temperature faster than the conduction model. The author, however, found that the overall grain kernel temperature and moisture predictions from the conduction model were better than that of the model.

The conduction model was used by Fasina et al. [55] to model temperature changes and moisture loss in barley grains subjected to infrared heating. The equations which take into account the internal and external resistances to transport processes are given by the following:

Mass transfer

$$\frac{\partial M}{\partial t} = \frac{1}{r^2}\frac{\partial}{\partial r} D_m r^2 \frac{\partial M}{\partial r} \tag{10}$$

Heat transfer

$$\rho c_g \frac{\partial T}{\partial t} = \frac{1}{r^2}\frac{\partial}{\partial r} k r^2 \frac{\partial T}{\partial r} \tag{11}$$

The initial and boundary conditions to Eqs. (10) and (11) are given as

$$M = M_i \qquad \text{at } t = 0,\ 0 < r \le R \tag{12}$$

$$T = T_i \qquad \text{at } t = 0,\ 0 < r \le R \tag{13}$$

$$-D_m \left.\frac{dM}{dr}\right|_s = h_m(M_s - M_{eq}) \qquad \text{at } t > 0,\ r = R \tag{14}$$

$$-kA_g \left.\frac{\partial T}{\partial r}\right|_s = q_r + h_c A_g(\theta - T_s) + \rho V h_{fg}\frac{\partial M}{\partial t} \qquad \text{at } t > 0,\ r = R \tag{15}$$

It is assumed that (a) agricultural materials are opaque to radiation and, therefore, impinged radiation is converted to heat at the surface of the material [7], (b) the flow of material in infrared equipment is in a thin or single-kernel layer, and (c) the kernel is spherical in shape.

The variable q_r in Eq. 15 is the heat radiated to the kernel from (a) the infrared heater directly above the grain bed and (b) the two side plates that enclose the space between the infrared heater and the grain bed. Equations (16) and (17) describe the contribution of each radiative term to the kernel heat and mass transfer phenomena are given below [56,57]; they state that the total resistance to radiation exchange between a surface (emitter or side plate) and the barley grain is comprised of the two surface resistances [the first and third terms of the denominator in Eqs. (16) and (17)] and the geometrical resistance (F_{ge}).

For the infrared heater,

$$q_{r2} = \sigma A_g (T_p^4 - T_s^4)\left(\frac{1-\varepsilon_g}{\varepsilon_g} + \frac{1}{F_{ge}} + \frac{1-\varepsilon_e}{\varepsilon_e(A_e/A_g)}\right)^{-1} \tag{16}$$

For the two side plates,

$$q_{r2} = 2\sigma A_g (T_p^4 - T_s^4)\left(\frac{1-\varepsilon_g}{\varepsilon_g} + \frac{1}{F_{gp}} + \frac{1-\varepsilon_p}{\varepsilon_p(A_p/A_g)}\right)^{-1} \tag{17}$$

F_{ge} and F_{gp} are the view or configuration factors between the grain and the heater and plate surfaces, respectively, and were obtained from the following relation for a small sphere (barley) and a rectangular plane (infrared emitter) [58]:

$$F_{gp} \text{ or } F_{ge} = \tan^{-1}\left(\frac{x(y - \cos\theta)}{\sqrt{(1 + x^2 + y^2 - 2y\cos\theta)}}\right) + \tan^{-1}\left(\frac{x\cos\theta}{\sqrt{(1+x^2)}}\right) \tag{18}$$

where $x = b/c$ and $y = a/c$. The constants a and b are the width and length of the rectangular plane, respectively. The constant c is the distance from the sphere to the rectangular plane.

4.2 Numerical Simulation

4.2.1 Mass Transfer

The mass transfer equation [Eq. (10)] can be rewritten as

$$\frac{\partial M}{\partial t} = D_m\left(\frac{\partial^2 M}{\partial r^2} + \frac{1}{r}\frac{\partial M}{\partial r}\right) + \left(\frac{\partial M}{\partial r}\right)^2 \frac{\partial D}{\partial M} \tag{19}$$

Using the central finite difference scheme (nomenclature given in Figure 8),

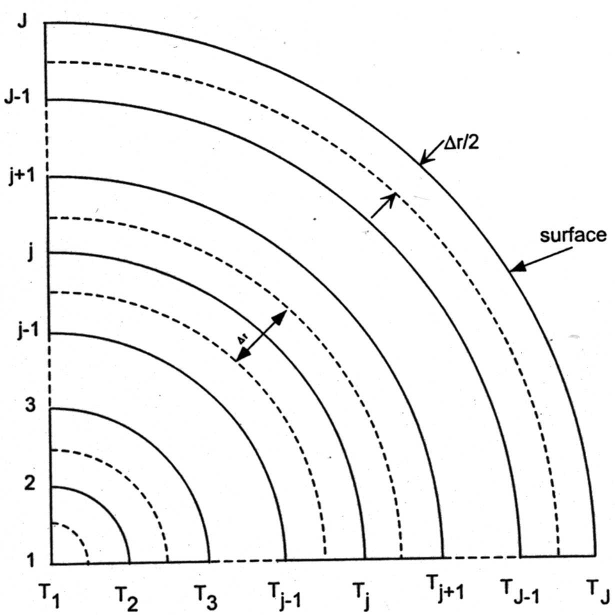

Figure 8 Nomenclature used for finite-difference formulation in spherical geometry.

we obtain,

$$M_{j+1}^{n+1} = M_j^n + \Delta t\left[D\left(a + \frac{b}{r}\right) + D'b^2\right] \tag{20}$$

where

$$a = \frac{M_{j-1}^n - 2M_j^n + M_{j+1}^n}{(\Delta r)^2} \tag{21}$$

$$b = \frac{M_{j+1}^n - M_{j-1}^n}{2\Delta r} \tag{22}$$

and

$$D' = \frac{\partial D}{\partial M} \tag{23}$$

When $r = 0$, Eq. (19) has a term with zero denominator. This makes the term $(1/r)(\partial M/\partial r)$ indeterminate. With the assumption that $\partial M/\partial r$ is a continuous function, l'Hospital's rule was therefore applied to obtain

$$\lim_{r\to 0} \frac{1}{r}\frac{\partial M}{\partial r} = \left.\frac{\partial^2 M}{\partial r^2}\right|_{r=0} \tag{24}$$

Substituting Eq. (24) into Eq. (19) with $\partial M/\partial r = 0$ at the center yields

$$\frac{\partial M}{\partial t} = 3D\frac{\partial^2 M}{\partial r^2} \tag{25}$$

At the center, $M_{j+1} = M_{j-1}$ and Eq. (25) takes the form

$$M_{j+1} = 6\Delta t D \frac{M_2^n - M_1^n}{\Delta r^2} \tag{26}$$

Simpsons's rule was used to obtain the average moisture concentration (M_{av}) using the relation

$$M_{av} = \frac{1}{(n-1)^3}\sum[(j-2)^2 M_{j-1} + 4(j-1)^2 M_j + j^2 M_{j+1}]$$

$$\text{for } j = 2, 4, 6, \ldots, n-2, n \tag{27}$$

A time step of 0.5 s and a size increase equal to one-tenth of the radius of the barley grain were used as step increase in the simulation program.

4.2.2 Heat Transfer

The heat transfer equation [Eq. (11)] was solved using the thermal resistance concept [59,60]. For a node d contained by the volume element ΔV_d, the steady-state energy balance equation can be written as

$$\sum_{j=1}^{n} \frac{T_i - T_d}{R_{jd}} = \rho c_g \Delta V_d \frac{dT}{dt} \tag{28}$$

The net heat flow to a point d from its surrounding nodes (denoted by j) is equal to the change in internal energy of the mass associated with the point. Applying Eq. (28) to any node j to $j-1$ gives

$$\frac{T_{j-1} - T_j}{B_{j-1,j}} + \frac{T_{j+1} - T_j}{B_{j+1,j}} = \rho c_g \Delta V_d \frac{dT}{dt} \tag{29}$$

where

$$B_{j-1,j} = \frac{\Delta r}{4\pi(j\Delta r - \Delta r/2)^2 k} = \frac{1}{4\pi j^2 \Delta r(1 - 1.2j)^2 k} \tag{30}$$

$$B_{j+1,j} = \frac{\Delta r}{4\pi(j\Delta r_\Delta r/2)^2 k} = \frac{1}{4\pi j^2 \Delta r(1 + 1/2j)^2 k} \tag{31}$$

and

$$\Delta V_j = 4\pi(j\Delta r)^2 \Delta r \tag{32}$$

Substituting Eqs. (30)–(32) into Eq. (29), we obtain the following:

$$(1-u)^2 T_{j-1}^n - 2vT_j^n + (1+u)^2 T_{j+1}^n = \kappa(T_j^{n+1} - T_j^n) \tag{33}$$

where

$$u = \frac{1}{2j}$$

$$v = 1 + \frac{1}{4j^2}$$

$$\kappa = \frac{\rho c_g (\Delta r)^2}{k\Delta t}$$

At the grain surface, the heat required to evaporate moisture from the surface is subtracted from the total heat flow into the surface node J. Applying Eq. (28) to Eq. (15) we obtain

$$\frac{T_{J-1} - T_J}{B_{J-1,J}} + h_c A_g(y - T_s) + q_r + \rho V h_{fg} \frac{\partial M}{\partial t} = \Delta V_J \rho c_g \frac{dT_J}{dt} \tag{34}$$

Substituting for $B_{J-1,J}$, A, V, and ΔV_J, Eq. (34) becomes

$$g_1 T_{j-1}^n + g_2 T_j^n + g_3 = \frac{\kappa}{2}(T_j^{n+1} - T_j^n) \tag{35}$$

where

$$g_1 = \left(1 - \frac{1}{2J}\right)^2$$

$$g_2 = -g_1 - \Delta \dot{r}\left(\frac{h_r - h_c}{k}\right)$$

$$g_2 = \Delta r\left(\frac{h_r}{k}\right) T_e - \Delta r\left(\frac{h_c}{k}\right) T_a + g_4 h_{fg}$$

$$h_r = \frac{q_r}{A_g(T_e - T_s)}$$

$$g_4 = \frac{J(\Delta r)^2 \rho}{3k} \frac{\partial M}{\partial t}$$

At the center where $r = 0$ and applying Eq. (28) yields

$$6(T_2^n - T_1^n) = \kappa(T_1^{n+1} - T_1^n) \tag{36}$$

The nodal temperatures required for numerical solution at time steps n and $n+1$ are therefore given by Eqs. (33), (35), and (36). The Crank–Nicolson method was used to numerically solve the equations. This method is a modification of the implicit method of the finite-difference solution in that stable solutions are obtained even though there are no restrictions on the time step used in the numerical algorithm [61]. Applying this method to Eqs. (33), (35) and (36) yields the following:

$$(1-u)^2 T_{j-1}^{n+1} - 2vT_j^{n+1} + (1+u)^2 T_{j+1}^{n+1} + (1-u)^2 T_{j-1}^n - 2vT_j^n + (1+u)^2 T_{j+1}^n = 2\kappa(T_j^{n+1} - T_j^n) \tag{37}$$

$$g_1 T_{j-1}^{n+1} + g_2 T_j^{n+1} + g_1 T_{j-1}^n + g_2 T_j^n + 2g_3 = \kappa(T_j^{n+1} - T_j^n) \tag{38}$$

$$T_2^{n+1} - T_1^{n+1} + T_2^n - T_1^n = \frac{\kappa}{3}(T_1^{n+1} - T_1^n) \tag{39}$$

Rearranging Eqs (37)–(39) to bring all the times for time $n+1$ to the left-hand side and those for time n to the right hand side, we obtain

$$\left(\frac{(1-u)^2}{2}\right) T_{j-1}^{n+1} + (-\nu - \kappa) T_j^{n+1} + \left(\frac{(1+u)^2}{2}\right) T_{j+1}^{n+1} = \left(-\frac{(1-u)^2}{2}\right) T_{j-1}^n + (\nu - \kappa) T_j^n + \left(-\frac{(1+u)}{2}\right) T_{j+1}^n \tag{40}$$

$$\frac{g_1}{2} T_{j-1}^{n+1} + \left(\frac{g_2 - \kappa}{2}\right) T_j^{n+1} = \frac{g_1}{2} T_{j-1}^{n} + \left(-\frac{g_2 - \kappa}{2}\right) T_j^{n} - g_3 \quad (41)$$

$$(-3 - \kappa) T_1^{n+1} + 3T_2^{n+1} = (-3 - \kappa) T_1^{n} - 3T_2^{n} \quad (42)$$

Equations (40)–(42) can be written in a matrix form as follows:

$$[A]\{T\}^{n+1} = [B]\{T\}^{n} + \{C\} \quad (43)$$

$[A]$ and $[B]$ are square banded matrices whose elements are the constants of Eqs. (40)–(42). The Gauss elimination procedure can be used to solve Eq. (43) to obtain a new set of temperature vector at any time step t.

4.3 Simulation Results

Figures 9 and 10 show the closeness of predicted to experimental data for the surface temperature and average moisture content of barley kernels subjected to infrared heating. Predicted temperature and moisture at the

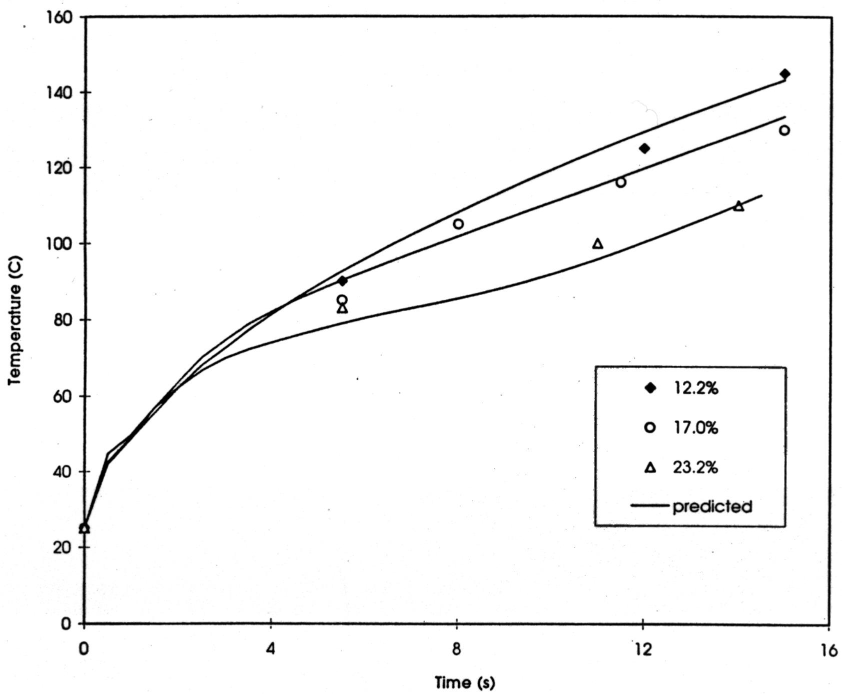

FIGURE 9 Comparison of predicted and experimental surface temperatures of infrared; heated hull-less barley at different initial moisture contents. (From Ref. 53.)

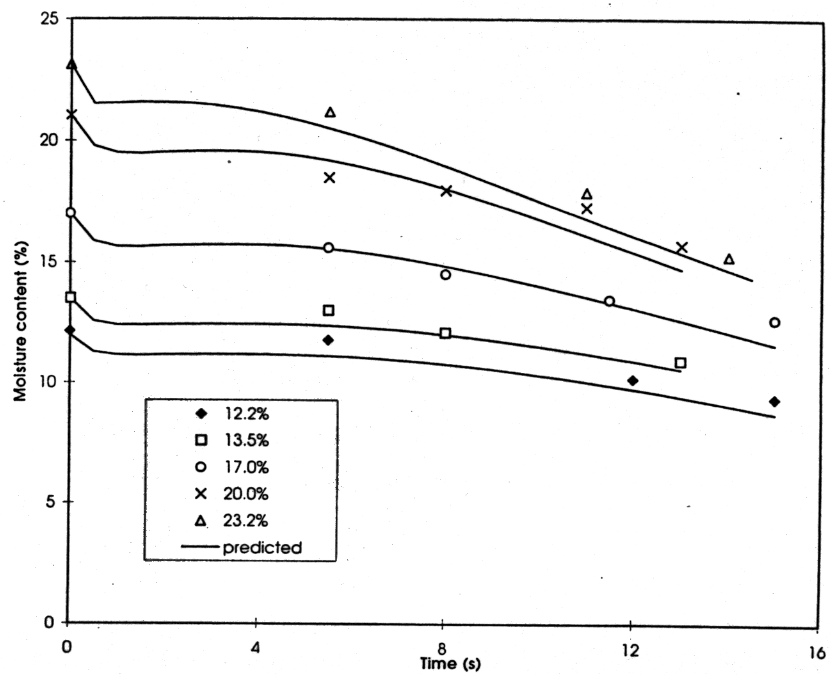

FIGURE 10 Comparison of predicted and experimental average moisture contents of infrared-heated hull-less barley at different initial moisture contents. (From Ref. 53.)

grain surface and center as affected by the initial moisture content are given in Figures 11 and 12. Exposure to infrared heat resulted in an immediate increase in kernel surface temperature. Surface and center temperatures were inversely related to moisture content due to the evaporative cooling effect. The difference in temperature between the surface and center of the kernels varied between 20°C and 45°C during the 15 sec of infrared exposure, supporting the applicability of infrared radiation to applications such as microbial decontamination and dehulling, which involves thermal and moisture treatment.

In order to compare the efficiency of heating of barley grains with infrared heating in comparison with hot-air (conventional) heating, we eliminated the radiative heat term (q_r) from Eq (15) and used hot-air temperature (θ) of 180°C. The value of the convective heat transfer coefficient was initially set at 30 W/m^2 K because this is numerically equal to the value of the radiative heat transfer coefficient that was calculated from Eq. (35) Figures 13 and 14 show that the time required for the grains to attain a

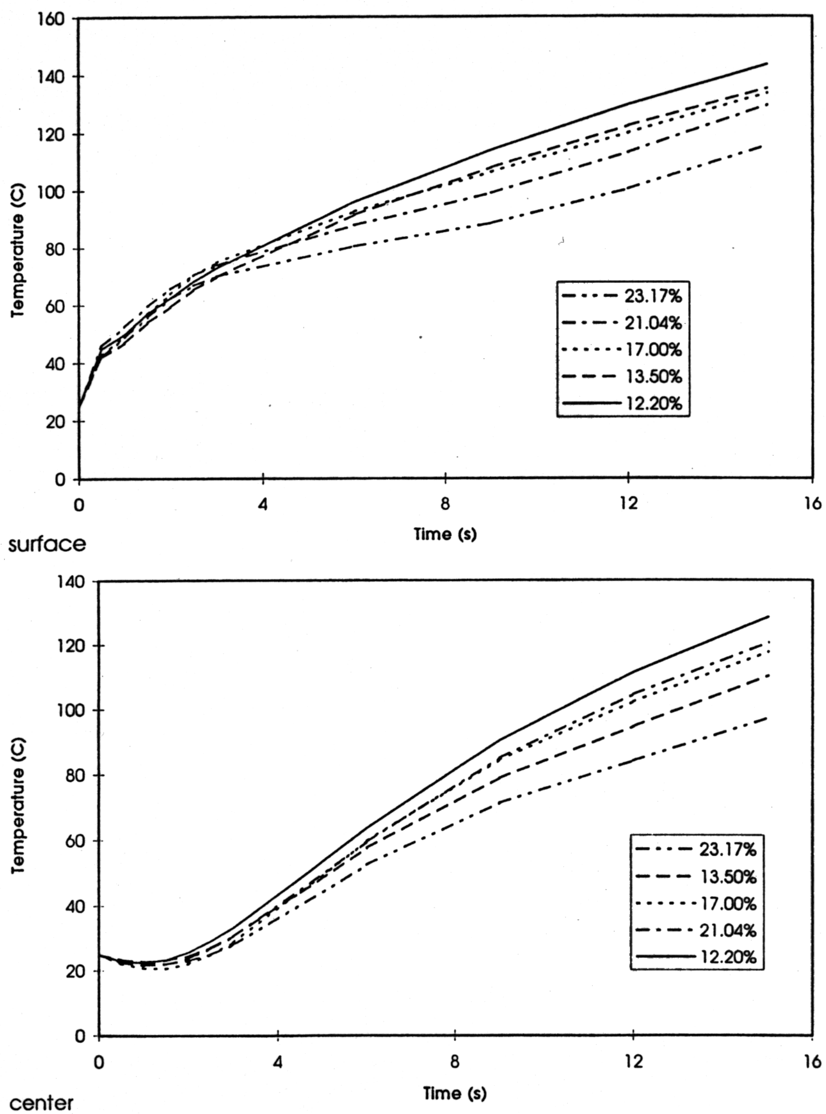

Figure 11 Effect of initial moisture content on predicted surface and center temperatures of hull-less barley. (From Ref. 53.)

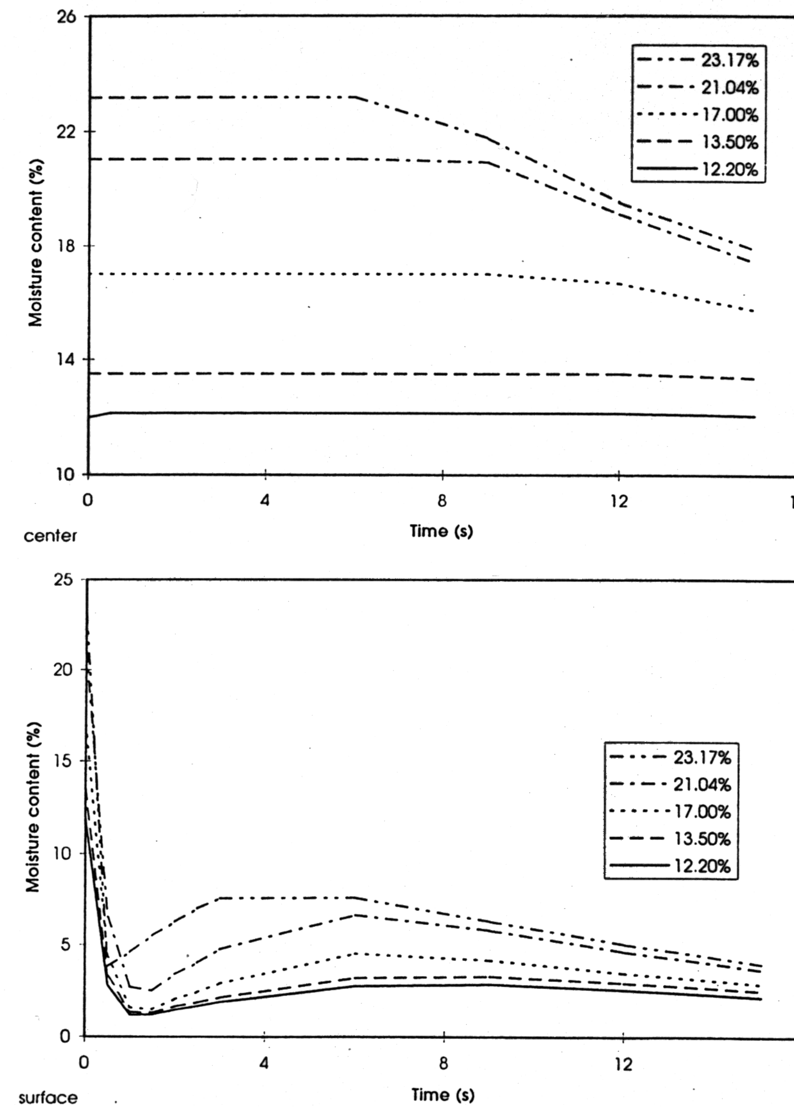

Figure 12 Effect of initial moisture content on predicted surface and center moisture contents of hull-less barley (From Ref. 53.)

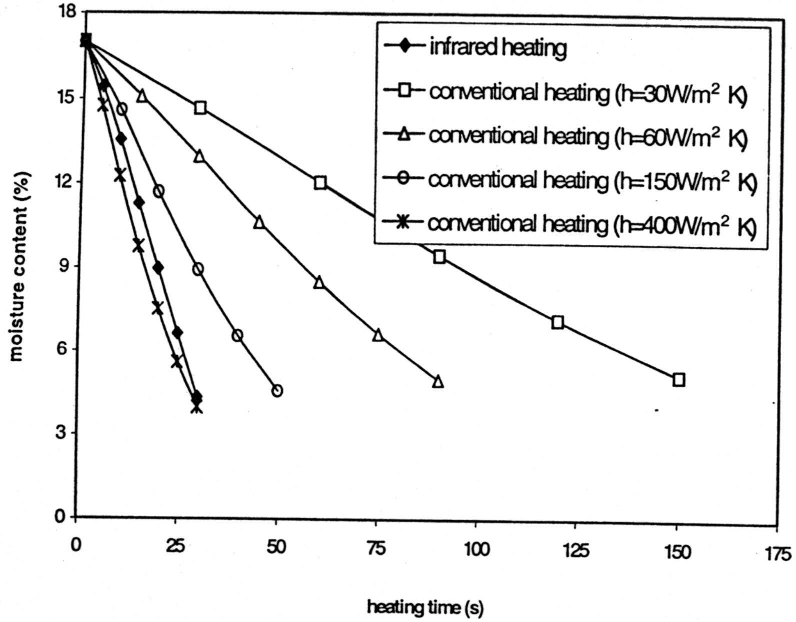

FIGURE 13 Average moisture content in barley grains when infrared heated (using emitter temperature of 850°C) in comparison with conventional heated grains using air temperature of 180°C.

surface temperature of about 170°C with hot-air heating is about 10 times of that required when the grains were infrared heated (30 sec). Similarly, the grains have to be hot-air heated for 150 sec before the average moisture content can be reduced to about 5 percentage points in comparison to 30 s required for infrared heating. Increasing the values of the convective heat transfer coefficient reduces the time required to attain the desired surface temperature of 170°C average moisture content of 5%. The value of the convective heat transfer coefficient required to achieve the desired temperature and moisture content was of 400 W/m^2 K. This is much higher than the h_c range of 50–200 W/m^2 K that is typically used in hot-air application [62]. This supports the claim of infrared heater manufacturers that energy is transferred much faster by infrared radiation. Dostile et al. [63] compared the an infrared dryer to that of convection dryer used for the drying of sheating panels and acoustic tiles. The hot air used for drying in the convection dryer was at a temperature of 170°C. Experimental results showed that it took 20 min to remove about 4 kg/m^2 of moisture from sheating panels using an infrared dryer in comparison to about 55 min for the conventional dryer. The difference in time required to remove 5 kg/m^2 of moisture from the acoustic tiles was also about 35 min (60 min for the infrared dryer and the 95 min for the convectional dryer).

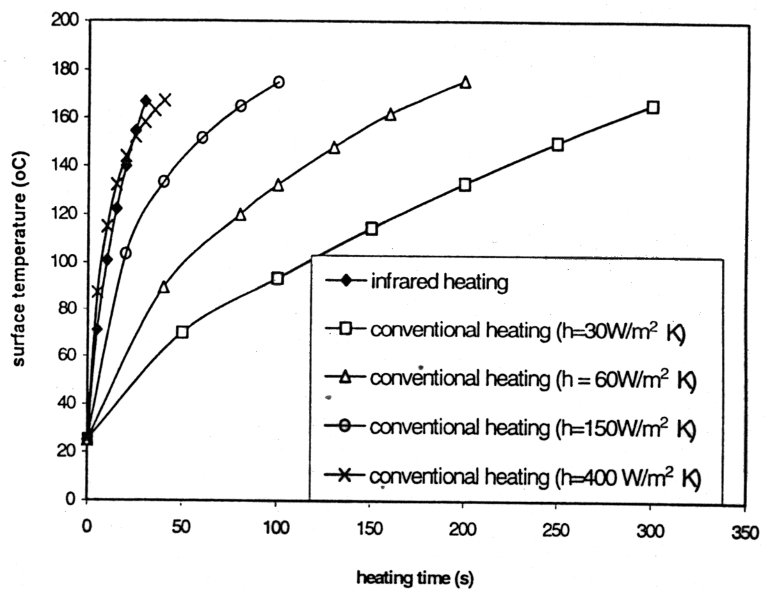

FIGURE 14 Surface temperature of barley grains when infrared heated (using emitter temperature of 850°C) in comparison with conventional heated grains using an air temperature of 180°C.

Figures 15 and 16 show the sensitivity of the infrared system to initial grain moisture content, infrared burner distance from grain bed, and infrared heater temperature. It can be summarized as follows.

1. Surface temperatures of grain were significantly increased with increases in burner temperature and with decreases in burner height.
2. At the end of 15 sec of exposure, kernel surface and center temperatures were respectively increased by approximately 115% and 110% for every 50°C increase in burner temperature and for every 0.04-m decrease in burner height from the grain bed.
3. The burner temperature and burner height did not significantly affect the rate and quantity of moisture change in barley subjected to infrared heating.

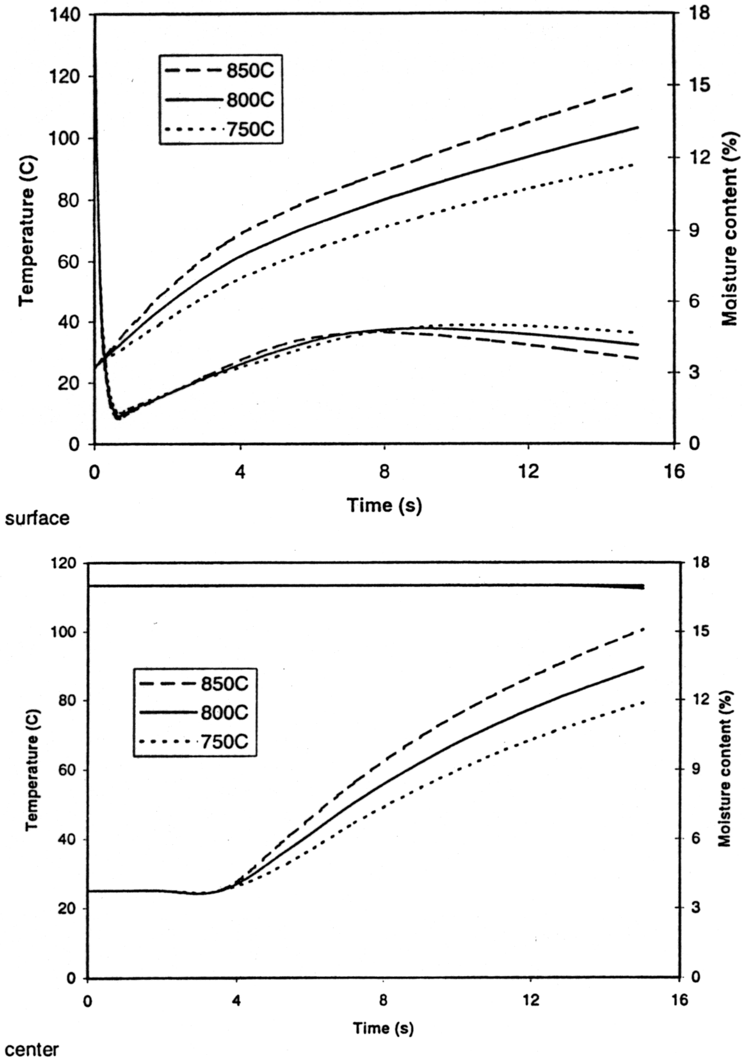

Figure 15 Effect of burner height on moisture content and temperature of hull-less barley. Burner temperature = 850°C; initial moisture content = 17% wet basis (wb) (From Ref. 53.)

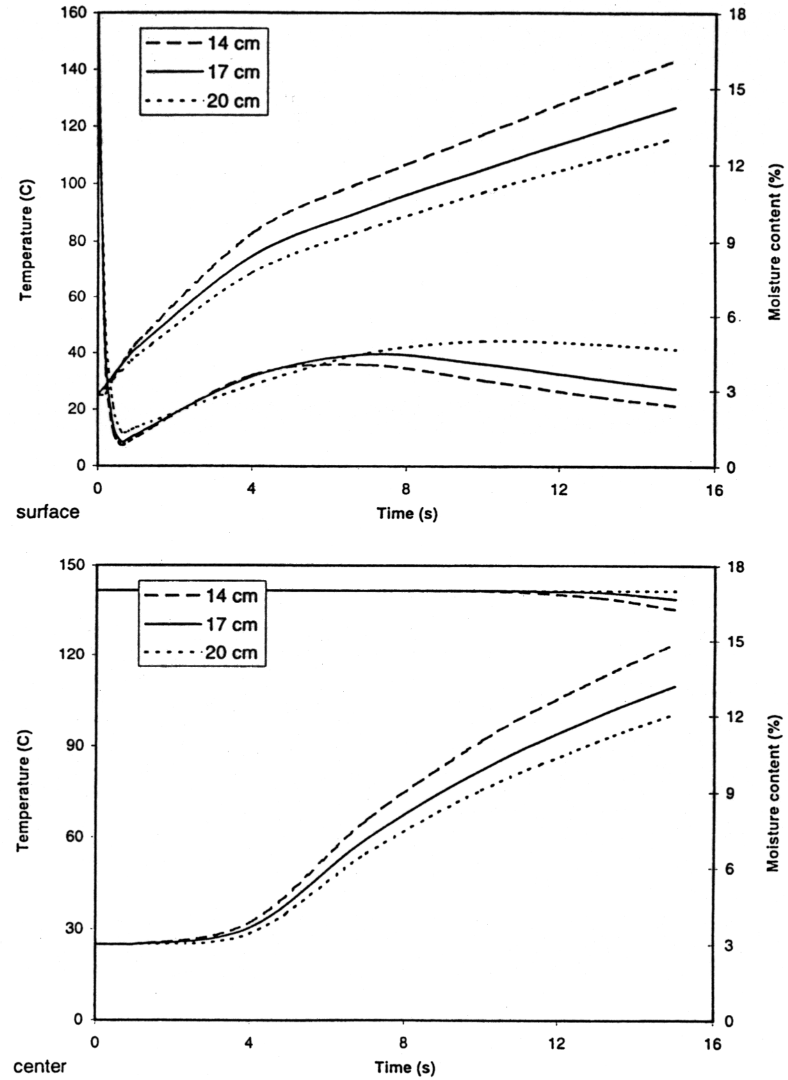

Figure 16 Effect of burner temperature on moisture content and temperature of hull-less barley. Height of burner = 20 cm; initial moisture content = 17% wb. (From Ref. 53.)

5 CLOSING REMARKS

In this chapter, we have shown the possibilities for the use of infrared heating in the processing of biological materials. In addition to using infrared heating as a means of moisture removal, the method can be used to alter the functional, chemical, and physical properties of cereal grains, legumes, and oilseeds, to reduce microbial load on surfaces of any material, and for rapid and routine determination of composition of food products. Even though the rapid rise in surface temperature has limited the possible application of infrared heating in the meat, milk, fruit, and vegetables industries, there is still room for the unique/novel use of this method in these industries such as in the drying/preservation of meat and fish especially due to its high heating rate in comparison to the conventional method of using hot air.

With increasing emphasis on biotechnology and production of transgenic seeds, infrared heating may be an alternative and quick way to conventional drying in order to achieve the purposes mentioned in the previous paragraph. However, further research is needed on the penetration of infrared radiation into biological material and the possible influence of infrared heating on the thermophysical properties of biological materials. The possibility of incorporating a heat-source term into Eq. (4) due to infrared penetration in biological materials should also be investigated. In addition, the models presented in this chapter need to be verified for other biological materials and for various configurations of infrared heating systems.

NOMENCLATURE

A	Surface area (m^2)
c	Specific heat (J/kg K)
D_m	Moisture diffusivity (m^2/sec)
E	Radiant energy emitted per unit area per unit wavelength interval ($W/m^2 \mu m$)
F	Configuration factor
h_c	Convective heat transfer coefficient (W/m^2 K)
h_{fg}	Latent heat of vaporization (J/kg)
h_m	Mass transfer coefficient (m/sec)
k	Thermal conductivity (W/m K)
M	Moisture concentration (%, dry basis)
q_r	Radiative heat component (W)
R	Particle distance (m)
r	Radial distance (m)
T	Temperature (K)

t	Time (sec)
V	Volume (m^3)
W	Radiant energy emitted per unit area (W/m^2)

Greek Letters

ρ	Density (kg/m^3)
σ	Stephan–Boltzman constant (5.6697×10^{-8} W/m^2 k^4)
ε	Emissivity
Δ	Change in parameter
λ_{max}	Wavelength for peak emission intensity (μm)
θ	Emitter temperature (K)

Subscripts

e	Infrared emitter
eq	Equilibrium
g	Grain
i	Initial
p	Side plate
s	Surface

REFERENCES

1. C Sandu. Infrared radiative drying in food engineering: A process analysis. Biotechnol Prog 2(30):109–119, 1986.
2. N Sakai, T Hanzawa. Applications and advances in far-infrared heating in Japan. Trends Food Sci Technol 5:357–362, 1994.
3. SG Il'yasov, VV Krasnikov. Physical Principles of Infrared Irradiation of Foodstuffs. Revised, Augmented and Updated Edition. New York: Hemisphere, 1991, p 397.
4. EA Arinze, GJ Schoenau, FW Bigsby. Determination of solar energy absorption and thermal radiative properties of some agricultural products. Trans ASAE 30(1):259–267, 1987.
5. C Strumillo, T Kudra Drying: Principles, Applications and Design. New York: Gordon and Breach Science, 1986, p 448.
6. B Halistrom, C Skjoldebrand, C Tragard. Heat Transfer and Food Products, New York: Elsevier Applied Science, 1988, p 263.
7. AS Ginzburg. Application of Infrared Radiation in Food Processing. London: Leonard Hill Books Strand, 1969, p 413.
8. C Ratti, AS Mujumdar. Infrared drying. In: AS Mujumdar, ed. Handbook of Industrial Drying, 2nd Edition, Revised and Expanded. New York: Marcel Dekker, Inc, 1995, pp 567–588.

9. DJ Zuilichem, K van Riet, W Stolp. An overview of new infrared radiation processes for agricultural products. In: LM Maguer, P Jelens, ed. Food Engineering and Process Applications, Transport Phenomena, Vol. 1, New York: Elsevier Applied Science, 1985, pp 595–610.
10. W Jones. A place in the line for the micronizer. Special Report, Micronizing Company (UK) Ltd., Framlinghem Suffolk, UK, 1992, pp 1–3.
11. RL Kirkpatrick. Infrared radiation for control of less grain borers and rice weevils in buck wheat. J Kans Entomol Soc 48:1549–1551, 1975.
12. RL Kirkpatrick, JH Bower, EW Tilton. Gamma, infrared and microwave radiation combinations for control of Rhyzopertha dominica in wheat. J Stored Prod Res 9:19–24, 1973.
13. M Kouzeh-Kanani, DJ van Zuilichem, JP Roozen, W Pilnik. A modified procedure for low temperature infrared radiation of soybeans. I. Improvement of nutritive quality of full-fat flour. Lebensm Wiss U Technol 14:242–244, 1981.
14. M Kouzeh-Kanani, DJ van Zuilichem, JP Roozen, W Pilnik. A modified procedure for low temperature infrared radiation of soybeans II. Inactivation of lipoxygenase and keeping quality of full-fat flour. Lebensm Wiss U Technol 15:139–142, 1982.
15. M Kouzeh-Kanani, DJ van Zuilichem, JP Roozen, W Pilnik. A modified procedure for low temperature infrared radiation of soybeans III—Pretreatment of whole beans in relation to oil quality and yield. Lebensm Wiss U Technol 17:39–41, 1984.
16. M Kouzeh-Kanani, DJ van Zuilichem, JP Roozen, W Pilnik, JR van Delden, W Stolp. Infrared processing of soybeans. Qual. Plant Foods Human Nutr 33:139–143, 1983.
17. Anon. Micronised soya flour produced commercially. South Afr Food Rev 2(2):22–23, 1975.
18. DJ van Zuilichem, AFB van der Poel. Effect of HTST treatment of Pisum Sativum on the inactivation of antinutritional factors. In: J Huismam, AFB van der Poel, JF Liener, eds. Recent Advances of Research on Antinutritional Factors in Legume Seeds. Wageningen, The Netherlands: Pudoc, 1989, pp. 263–267.
19. I. Bozovic. Testing the suitability of methods of evaluating the quality of processed soybean. Arhiv Za Pojoprivredne Nauke 52(187):255–270, 1991.
20. Anon. New infrared machine for cocoa processing. Confect Product 47(6):308–309, 1981.
21. M van Liere. Process for treating raw soybeans. US Patent 4810513, 1989.
22. RL Anderson. Effects of steaming on soybean proteins and trypsin inhibitors. J Am Oil Chem Soc 69(12):1170–1176, 1992.
23. S Cenkowski, FW Sosulski. Physical and cooking properties of micronized lentils. J Food Process Eng 20(3):249–264, 1997.
24. M Kouzeh-Kanani, DJ van Zuilichem, JP Roozen, W Pilnik. Infrared processing of maize germ. Lebensm Wiss U Technol 17:237–239, 1984.
25. OO Fasina, WD Ziehl, RT Tyler, MD Pickard. Adaptation of micronization to the development of functional food ingredients from waxy barley and pulses, including the adaptation and testing of a small scale, gas fired micronization unit. Project No. 32232 p. Report to submitted to the National Research Council of Canada, 1997 pp 95.

26. GH Zeng, OO Fasina, FW Sosulski, RT Tyler, Nitrogen solubility of cereals and legumes subjected to micronization. J Agric Food Chem 46(10):4150–4157, 1998.
27. DE Blendford. Potential applications of micronizing in food processing. Confect Manuf Market 16(4):3–5, 7, 1979.
28. I Rosenthal. Electromagnetic Radiations in Food Science. New York: Springer-Verlag, 1992, p. 244.
29. BA Rusnak, CL Chou, LW Rooney. Effect of micronizing on kernel characteristics of sorghum varieties with different endosperm type. J Food Sci 45(6): 1529–1532, 1980.
30. JA Collier. The application of recent technical advances to commercial production of brewery materials. Brewer 59:507–510, 1973.
31. JA Collier. Trends in UK usage of brewing adjuncts. Brewing Distilling Int 16(3):15–17, 1986.
32. OO Fasina, RT Tyler, MD Pickard, GH Zheng. Infrared heating of hulless and pearled barley. J Food Process Preserv 23:135–151, 1999.
33. TU Lawrence. Some effects on the growth and composition on the carcass of the bacon pig of feeding micronized or ground maize or barley based diets to give three different digestible energy intakes. Livestock Prod Sci 4(4):343–353, 1977.
34. TU Lawrence. An evaluation of the micronization process for preparing cereals for the growing pigs. II. Effects on growth rate, food conversion efficiency, and carcass characteristics. Anim Product 16(2):109–116, 1973.
35. JC Aimone, DG Wagner. Micronized wheat. I. Influence of feedlot performance digestibility, VFA and lactose levels in cattle. J Anim Sci 44(6):1088–1095, 1977.
36. SY Shiau, SP Yang. Effect of micronizing temperature on the nutritive value of sorghum. J Food Sci 47(3):965–968, 1982.
37. D Meyer, H Zwingelber, AW El-Baya, Experimental production of oat flakes with the micronizer. Getreide Mehl Brot 36(10):259–263, 1982.
38. G Spicher, H Zwingelberg. The micronizer—Equipment for reduction of the microflora in wheat bran. Getreide Mehl Brot 35(11):296–299, 1987.
39. CW Glennie, KH Daiber, RJN Taylor. Reducing the tannin content in sorghum grain by heat. South Afr Food Rev 9(3):51–55, 1982.
40. TM Afzal, T Abe. Thin layer infrared radiation drying of rough rice. J Agric. Eng Res 67(4): 289–297, 1997.
41. WR Lein, WR Fu. Small fish dehydration by far infrared heating. Food Sci Taiwan 24(3):348–356, 1997.
42. JS Townsend, S Cenkowski, M Friesen-Fischer. The thermal effects of high intensity infrared radiation on fresh lettuce leaves. Proceedings of an International Conference of Harvest and Postharvest Technologies for Fresh Fruits and Vegetables, Guanajuato, Mexico, 1995, pp 268–275.
43. R Metussin, I Alli, S Kermasha. Micronizaton effects of composition and properties of tofu. J Food Sci 57(2):418–422, 1992.

44. C Friedrich. Browning of foods. New applications for IR techniques. Process 1089:40, 1993.
45. JF Metzger, WE Muir. Computer model of two-dimensional conduction and forced convection in stored grain. Can Agric Eng 25(1):199–225, 1983.
46. KQ Stephenson, GW McKee. Accelerated drying of seeds with infrared radiation. Trans ASAE 229–231, 1964.
47. CW Hall. Theory of infrared drying. Trans ASAE 5(1):14–16, 1962.
48. H Kuang, J Thibault, BPA Grandjean. Study of heat and mass transfer during IR drying of paper. Drying Technol 12(3):545–575, 1994.
49. M Fortes, MR Okos. A non-equilibrium thermodynamics approach to transport phenomena in capillary porous media. Trans ASAE 24:760–80, 1981.
50. S Sokhansanj Improved heat and mass transfer models to predict grain quality. Drying Technol 5:511–525, 1987.
51. OO Fasina, S Sokhansanj. Estimation of moisture diffusivity coefficient and thermal properties of alfalfa pellets. J Agric Engng Res 63:333–344, 1996.
52. M Parti. Selection of mathematical models for drying grains in thin layers. J Agric Eng Res 54:339–353, 1993.
53. J Irudayaraj, K Haghighi, RL Stroshine. Finite element analysis of drying with application to cereal grain. J Agric Eng Res 53:209–229, 1992.
54. AV Luikov. Heat and Mass Transfer in Capillary Porous Bodies. Oxford: Pergamon Press, 1966, p 523.
55. OO Fasina, RT Tyler, MD Pickard. Modeling the infrared heating of agricultural crops. Drying Technol 16(9&10):2065–2082, 1998.
56. FP Incropera, DP DeWitt Fundamentals of Heat and Mass Transfer, 4th ed. New York: John Wiley & Sons, 1996, p 886.
57. MN Ozisik. Radiative Transfer and Interactions with Conduction and Convection. New York: John Wiley & Sons, 1973, p 575.
58. LD Albright. Environmental Control for Animals and Plants. St. Joseph, MI: American Soc of Agricultural Engineers, 1990.
59. MN Ozisik. Heat Transfer—A Basic Approach. New York: McGraw Hill, 1985.
60. S Sokhansanj, DM Bruce. Finite difference solutions of heat conduction and moisture diffusion equations in single kernel grain drying. Divisional Note 1351, National Institute of Agricultural Engineering, Silsoe, Bedford, UK, 1986.
61. PK Chandra, RP Singh. Applied Numerical Methods for Food and Agricultural Engineers. Boca Raton, FL: CRC Press, 1994.
62. RP Singh, DR Heldman. Introduction to Food Engineering, 2nd ed. New York: Academic, 1993.
63. M Dostie, JN Seguin, D Maure, QA Ton-That, R Chatigny. Preliminary measurements on the drying of thick porous materials by combination of intermittent infrared and continuous convection heating. In: AS Mujumdar, MA Roques, eds. Drying '89. New York: Hemisphere, 1989, pp. 513–519.